SARS-CoV-2-Main Protease Inhibitor by the Active Alkaloid: An *in silico* Molecular Docking and Dynamic Approach

Nurul Hoda Khan[1], Shukra Raj Regmi[1*], Narendra Prakash Shawd[1], Padam Raj Joshi[1], Savita Dhungana[1], Ram Prasad Baral[2], Rameshwar Adhikari[3]

[1]Central Department of Biological and Chemical Sciences
Graduate School of Science and Technology, Mid-West University, Birendranagar, Surkhet, Nepal
[2]Central Department of Chemistry, Tribhuvan University, Kritipur, Kathmandu, Nepal
[3]Research Centre for Applied Science and Technology (RECAST), Tribhuvan University, Nepal
**Correspondance: shukra.regmi@mu.edu.np; Ph. 9849024059*

Keywords

SARS-CoV-2
Withanone
Molecular docking
6LU7-Withanone complex

Received: 13 November 2024
Revised: 28 November 2024
Accepted: 05 December 2024

ISSN: 3059 - 9687

Abstract

The rampant outbursts of alpha, beta, gamma, delta, omicron, and their subvariants were so vehement that the millions of dramatic deaths forced us to think about a potential inhibitor against SARS-CoV-2 main protease in the future. In the present research work, we have searched bioactive compounds from *Withania somnifera, Ocimum sanctum,* and *Tinospora cordifolia* to inhibit the replication of main protease M^{pro} through *in-silico* molecular docking and dynamic approach. The ADMET evaluation was applied to confirm the absorption, distribution, metabolism, excreation, and toxicity parameters based on Lipinski's rule of five. The free energy change for the Withanone docked complex is found -8.50 KCal/mol, -7.82 KCal/mol for Tetrahydropalmatine, -7.77 KCal/mol for Isocolumbin and -7.50 KCal/mol for Magnoflorine. Similarly, their RMSD and RMSF spectra are more stable than the main protease inhibitory capacity of Dexamethasone, Chloroquine, and Remdesivir prescribed in SARS-CoV-2. The docked complex of the main protease with Withanone is a very strong and stable with conventional hydrogen bonding of bond lengths 1.76 Å (ARG A: 105), and 2.16 Å (GLN A: 107). The molecular dynamic results revealed that the docked complex is stable up to 100 ns for RMSD, and 10 ns running for RMSF. The finding shows that the inhibitory potential of Withanone, Tetahydropalmatine, Isocolumbin, and Magnoflorine are comparatively high for SARS-CoV-2, and can be effectively used against SARS-CoV-2 infection without side effects. Based on the investigation, it could be recommended that further tests and trials are required to confirm the efficacy of the drug.

Introduction

Novel COVID-19 was first reported in Wuhan China as a pandemic agent having several magnitudes infectious than any other previous recorded cases. The COVID-19 pandemic was so severe that millions of cases were reported globally with an unexpected mortality rate. The Johns Hopkins University recorded that globally more than 20 million cases were registered with a million death cases (Dong *et al.*, 2022). The WHO declared the COVID-19 pandemic as a global emergency in 2019 AD. The RNA-based etiological agent that causes infectious dispersion through a medium is commonly known as Corona (SARS-Cov-2). The main enzyme of the virus M^{pro} plays a vital role in

replication and transcription in a host cell as a source of rampant outbursts (Jin *et al.*, 2020).

Medical diagnoses revealed that it causes upper and lower respiratory tract infections like distress, mild pneumonia, bronchitis, neuro disorders, multiple organ failure, septic shock, and ultimately death (Krishnan *et al.*, 2021). It is a single-stranded RNA matrix nucleoprotein having a diameter below 120 nm, and the main structural components are spike glycoprotein (S-Protein) for binding the ACE2 receptor of the host, envelope protein membrane (E-protein) for assembly and release, and nucleocapsid (N-protein) which encapsulate the genome and helps in replication and transcription (Wrapp *et al.*, 2020), (Yadav *et al.*, 2021). The single-stranded RNA coronavirus belongs to genera Betacoronavirous including SARS-CoV, MRRs-CoV, and SARS-CoV-2, which contain ORFs as genomic constituents, and the required proteins were transcript from sgRNAs that are found in 3' terminus of the strand. Typically, COVID-19 is distinct due to its genomic and phenotypic modification as a potential viral pathogen reported in the pandemic (Brant *et al.*, 2021), (Mousavizadeh & Ghasemi, 2021). Since the first recorded case of COVID-19 virus, it has been muted several times as alpha, beta, gamma, delta, and Omicron. The emerging mutant infectious COVID-19 and its subvariant (BA.1 & BA.2) have shown remarkable genomic recombination leading to an evolution of SARS-CoV-2. The amino acid mutation in the delta spike protein was detected as a possible recombination from 'Omicron' and 'Deltacron' subvariants (Ou *et al.*, 2022). The genomic sequence has revealed that the Delta variant (B.1.617.2) and Omicron (B.1.1.529) were rapidly dispersed as an infectious agent due to genomic modification, and their proper adaptation in host cells. The report has shown that the genomic sequence obtained from the Wuhan-Hu-1 strain of region TRS (CUAAC or ACGAAC) has been modified in recent sequencing. It is reported that the spike protein of Omicron has shown 30 mutations with a higher alpha-helix shape than the Delta variant (Ahmad *et al.*, 2022).

The governments of the different countries used a common practice of isolation and vaccination as preventive measures against the infectious COVID-19. The technological innovations have launched vaccines, categorized as intact target vaccines, proteins, viral vectors, and nucleic acid. The reports show the dire applications of high-efficiency RNA and viral vector-based vaccines implemented for trials (Nakagami, 2021). The synthetic peptides or recombinant protein-based vaccines are found effective against SARS-CoV-2. The vaccines based on mRNA, viral vector, and inactivated virus vaccine members are approved worldwide (Bayani *et al.*, 2023). Reports have shown that the spike protein epitome (C662-C671) of SARS-CoV-2 is used to develop broad-spectrum vaccines against the viral infection. The sequencing of amino acid of C662-C671in SARS-CoV-2 is observed over the other variants of the virus-like Omicron. Such conservation can pave the way for genomic replication and translation for new vaccine discoveries (Markosian *et al.*, 2022). Furthermore, The role of micronutrients like Vitamin A, B, C, and D, including Zn, Cu, and Mg also shows several clinical impacts on SARS-CoV-2 (Altooq *et al.*, 2022). The non-therapeutic approach may also be found effective through their novel capability against the viral mutation for the development of vaccines. Different techniques were launched based on peptide-

targeted and adeno-associated phases for targeted spike protein mainly capsid pVIII shows quick response on injecting mice through aerosolization. The protein on minor capsid pIII transport towards the circulation of the epithelium of the lungs shows an antibody response. Similarly, inducing spike protein-specific antibodies shows a quick response in the epithelium of mice. These techniques can be useful to generate vaccine prototypes (Lubin *et al.*, 2021). The *in vitro* transcription of mRNA sequence-based vaccine is a cost-efficient and flexible method against viral genetic transcription. The mRNA-based vaccines may be the pivotal discovery in pharmaceutical companies against SARS-CoV-2 in the future (Weng *et al.*, 2020). Technological advancement also explores the Nanomaterials against the viral protease because carriers are safe, effective, and promising like the treatment of other viral diseases (Yasamineh *et al.*, 2022). Ayurvedic Vasma contains the fine nanoparticles of metals like Au, Ag, Zn, Cu, Fe, etc (S. Regmi *et al.*, 2015). The nanostructure particles of these metals have a strong tendency to disrupt the nucleocapsid of SARS-CoV-2 variants. Different compositions and categorical Ayurvedic Vasma can be used to reduce TNFα levels, interleukins, and interferons due to their antiviral, anti-inflammatory, immunomodulatory, and adjuvant activities (Sarkar & Das Mukhopadhyay, 2021).

Ayurveda medicines are found effective against SARC-CoV-2 than those patients who took both Allopathic and Ayurveda medicine together. Ayurveda medicines were safer to use without side effects (Balkrishna *et al.*, 2021). Plants are the major sources that contain alkaloids, flavonoids, polyketides, Phonoloids, and triterpenoids which are effectively used as potential drugs for antiviral, antibacterial, antifungal, and many therapeutic purposes. The bioactive phytochemicals are found effective, reported in traditional Ayurveda treatment (Alam *et al.*, 2021). The key targets for the virus in the host cell are ACE2 and TMPRSS2. The viral activity can be reduced by the action of Ayurvedic medicinal plants like *Oscimum sanctum*, and *Piper longum* which contain high phytochemicals and their medicinal alkaloids that interact effectively against the particular host cell ACE2 and TMPRSS2 to inhibit their activity (Jindal & Rani, 2023). Likewise, (Shree *et al.*, 2022), reported that Withanoside V extracted from *Withania somnifera* effectively inhibits M^{pro} of SARS-CoV-2 with a high docking score. The Tinocordiside extracted from *Tinospora cordifolia* effectively inhibits the main protease through *in silico* approach. Similar reports were obtained for the Vinenin extract from *Ocimum sanctum*. The E protein is related to the replication of protease in the virus which is effectively inhibited by the extract obtained from *Withania somnifera* (Abdullah Alharbi, 2021). In the present research study, we have selected three different Ayurvedic plants *Withania somnifera*, *Ocimum sanctum*, and *Tinospora cardifolia*, and their vital active compounds for molecular docking against the main protease of SARS-CoV-2.

Materials and Methods

Tools and techniques in Molecular docking

The authentic computer-based software like PyMol (3.0) was used for 3D molecular visualization of protein and ligand analysis. Biovia discovery visualizer (21.1) was used for interactive 2D and 3D visualization of the molecular system. Avogadro Software (1.0) was used for molecular edition and modification.

Similarly, ADFR (V 2.7) was used for molecular docking, and VMD (Visual Molecular dynamics-1.9.4α53) was used for molecular modeling. Furthermore, server-based programs like ADMET prediction, protein topography, active site prediction through CASTp 3.0, NAD for molecular dynamics, and CABS-flex 2.0 for docked complex fluctuation.

6LU7 Chain-A Protein Preparation

The main protein of Mpro Omicron was loaded from RCSB.org as PDB ID 6LU7 in 'FASTA' format. The protein was sequenced on PyMol (3.0) by removing the reaming chain except A from the protein structure. The process was followed by eliminating ligands, water molecules, and ions. The clean protein chain A residue was made defectless by adding polar hydrogen, minimizing energy, and applying a gradient force field. The geometry of the protein was stabilized on Avogardo software (1.0) by maintaining pH = 7.4. The protein was prepared by converting the protein databank file 'FASTA' into 'pdb' to 'pbdqt' by issuing the following commands in the window power cell.

‡prepare_receptor –r .\6LU7_M^{pro}.pdb –o .\6LU7_M^{pro}.pdbqt

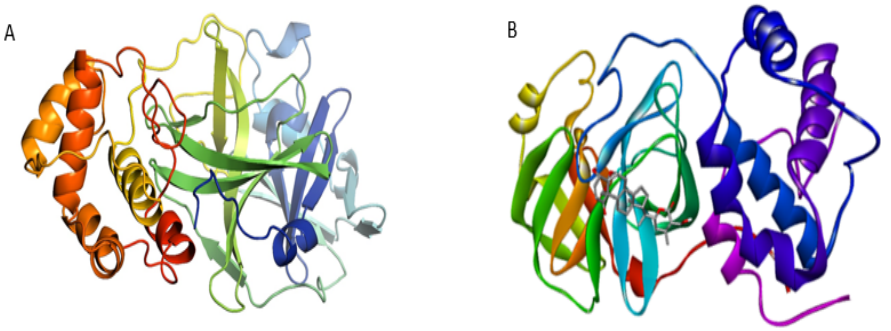

Fig. 1. *The main protease of COVID-19 (6LU7), the image is refined in PyMol and obtained from RCSB PDB, 6LU7 Withanone complex showing chain segment and bonding.* Source: RCSB.org, (Bugnon *et al.*, 2024)

3D Visualization and Edition of Protein in Avogadro 1.1

Avogadro 1.1 was used in the present research work to analyze and visualize 6LU7 M^{pro} loaded from RCSB.org. and PubChem. Its potential plugin mechanism on drug design to extract common databases like the 'CML' format has made Avogadro 1.1 a vital software (Hanwell *et al.*, 2012).

Ligands Preparation

The brief survey report has shown that some ayurvedic plants like *Osimum sanctum, Withania somnifera,* and *Tinospora cordifolia* are found to be affected in SARS-CoV-2. In the present study, we have selected some bioactive compounds from them. The ligands were prepared by loading 'Sdf' file format from the PubChem database with their PubChem ID. The following power cell command was issued to convert 'pdb' into the 'pbdqt' file format.

‡prepare_ligand -1 .\Ligand.pdb –o .\Ligand.pdbqt
‡prepare_ligand -1 .\Withanone.pdb –o .\Withanone.pdbqt
‡prepare_ligand -1 .\Azithromycine.pdb –o .\Azithromycine.pdbqt
‡prepare_ligand -1 .\Hydroxychloroquine.pdb –o .\Hydroxychloroquine.pdbqt
‡prepare_ligand -1 .\Dexamethazone.pdb –o .\Dexamethazone.pdbqt
‡prepare_ligand -1 .\PolymyxinB1.pdb –o .\PolymyxinB1.pdbqt
‡prepare_ligand -1 .\Remdesivir.pdb –o .\Remdesivir.pdbqt
‡prepare_ligand -1 .\Neomycine.pdb –o .\Neomycine.pdbqt
‡prepare_ligand -1 .\Gentamycine.pdb –o .\Gentamycine.pdbqt
‡prepare_ligand -1 .\Isocholumbin.pdb –o .\Isocholumbin.pdbqt
‡prepare_ligand -1 .\Tetrahydropalmatine.pdb –o .\Tetrahydropalmatine.pdbqt

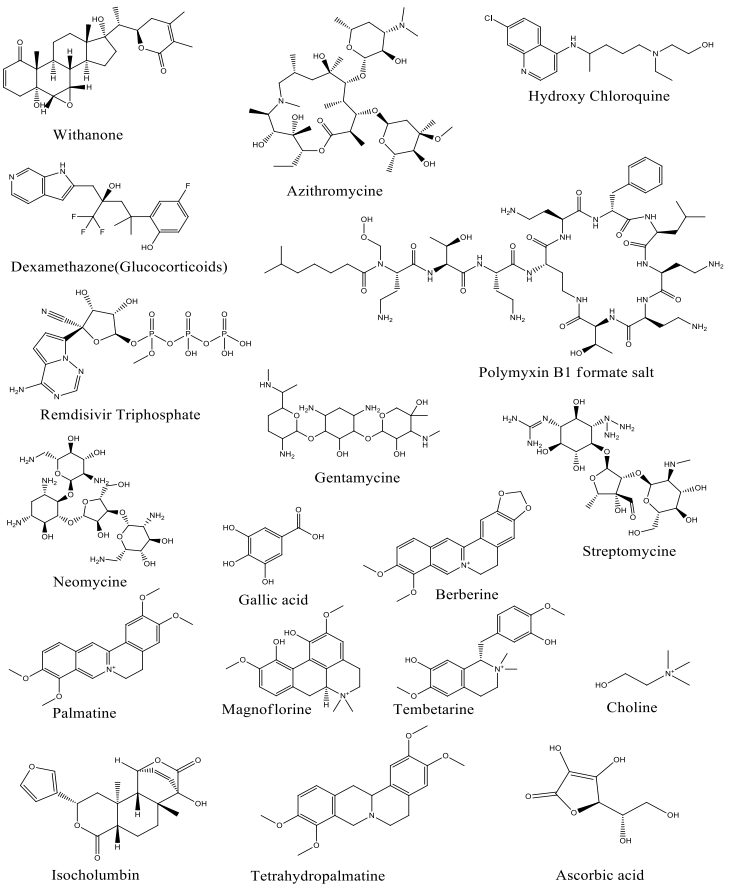

Fig. 2. *The structure of different bioactive compounds was obtained from the PubChem database and modified on ChemDraw 12.0 Ultra.*

ADMET Evaluation for Ligand in ADMET Lab 3.0

The drug-like properties and toxicity are evaluated on ADMET Lab 3.0. ADMET screening was performed to observe the features of ligand-based absorption, distribution, metabolism, excretion, and toxicity. The evaluation of each ligand screened based on Lipinski,s rule of five including some selected circumstances like molecular weight (100-600), LogP (0-3 logmol/l), LogS (-4 to 0.5 log mol/l), LogD7.4(1-3 log mol/l), nHA (0∼12), nHd (0∼7), TPSA (-4-0.5logmol/l), nRot (0-11), nRing (0-18), nHet (1-15), fChar (-4 – 4), nRing (0-30) (Xiong *et al.*, 2021).

Molecular Docking in AGFR 1.2

Molecular docking was carried out on AGFR 1.2. The refined protein and ligand on the 'pdbqt' file format were loaded on the software to get the target file. It was generated by keeping the fixed paddling (2.0) and appropriate grid box size. At least 15 flexible residues were selected for the docking with the receptor protein. The CASTp determined the active sites of the protein.

‡adfr -l Withanone.pdbqt -t 6LU7_Withanone.trg –MU flexRes --nbRuns 8 --maxEvals 50000 -O --seed 1
‡adfr -l Azithromycine.pdbqt -t 6LU7_Azithromycine.trg –MU flexRes --nbRuns 8 --maxEvals 50000 -O --seed 1
‡adfr -l Dexamethazone.pdbqt -t 6LU7_Dexamethazone.trg –MU flexRes --nbRuns 8 --maxEvals 50000 -O --seed 1
‡adfr -l Remdesivir.pdbqt –t 6LU7_Remdesivir.trg –MU flexRes --nbRuns 8 --maxEvals 50000 -O --seed 1
‡adfr -l Neomycine.pdbqt -t 6LU7_Neomycine.trg –MU flexRes --nbRuns 8 --maxEvals 50000 -O --seed 1
‡adfr -l PolymyxinB1.pdbqt -t 6LU7_PolymyxinB1.trg –MU flexRes --nbRuns 8 --maxEvals 50000 -O --seed 1
‡adfr -l Gentamycine.pdbqt -t 6LU7_Gentamycine.trg –MU flexRes --nbRuns 8 --maxEvals 50000 -O --seed 1
‡adfr -l Tembetarine.pdbqt -t 6LU7_Tembetarine.trg –MU flexRes --nbRuns 8 --maxEvals 50000 -O --seed 1
‡adfr -l T-palmatine.pdbqt -t 6LU7_T-palmatine.trg –MU flexRes --nbRuns 8 --maxEvals 50000 -O --seed 1

Interactive 2D and 3D Visualization in Discovery Studio 21.1.0

The docked complex in 'pdb' format was observed in Discovery studio. The 2D and 3D interaction of donor receptor complex was observed with high resolution with hydrogen bonding, pi-alkyl bond, alkyl-alkyl interaction, and their depiction with bond distance.

VMD and CABS-flex 2.0 For RMSD and RMSF

The protein structure docked with ligand fluctuation is carried out in a server-based CABS-flex web server. This server with an inexpensive computational framework determines the protein structure and its function relationship. The customizable distance, contact map, multimeric protein structure, and simulation parameters are determined through an enhanced web server interface. The RMSD values for the docked complex were determined through the generation of 'pdb' and 'psf' files, followed by the solvation box. In the present research work, we have specified the box size Minimum (X=2, Y=2, and Z=2), and Maximum (X=100, Y=100, and Z=100). Similarly, the box padding was issued as Min (X=5, Y=5, and Z=5), and Max (X=6, Y=6, and Z=6). The following command was issued to generate log files for NAMD trajectory and NAND plots. The executed command was given as:

\6LU7>tclsh .\maxmin_new.tcl and >nand2 script.txt > simul_log.log.

Result and Discussion

Surface Topography of Protein in CASTp 3.0

X-ray diffraction technique has shown its resolution of 2.16 Å, R-value free 0.235, R-value work 0.202, and observed R-value 0.204. The molecular weight of the protein is 34.51 Kda. The volume of the receptor side chain A is 319.370 $Å^3$, the surface area is 315.125 $Å^2$. It was found that the total AA residue Chain A is 306 with residue active sites are 81.

Table 1. Active site prediction for targeted protein 6LU7 with CASTp 3.0 server.

Protein	Pocket ID Chain	Volume (SA) $Å^3$	Area (SA) $Å^2$	Total Surface Weight kDa	X-ray diffraction Resolution Å	Total AA residue in Chain A	AA residue at the predicted active site
6LU7	A	319.370	315.125	35.51	2.16	306	81

Source: (Tian *et al.*, 2018), CASTp 3 Server

Table 2. The surface topography of protein 6LU7-Chain A Sequence shows genomic code for SARS-CoV-2 in CASTp (POCID:1: J_66b6435516DAE).

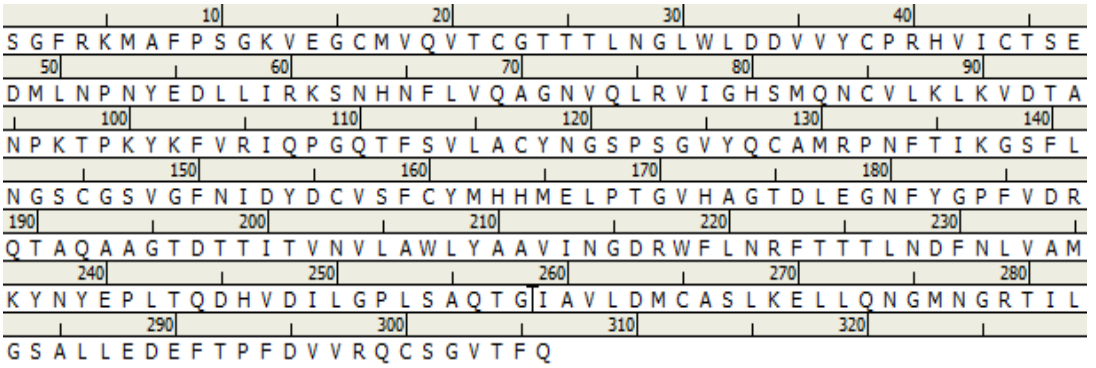

The amino acid residue presents in Chain A, PocID 1. are: Sequence ID 24 (THR, THR, THR), 25 (THR, THR, THR), 26 (THR, THR, THR), 27 (LEU, LEU), 41 (HIS, HIS, HIS, HIS, HIS, HIS)
44 (CYS), 45 (THR, THR), 46 (SER, SER, SER), 49 (MET, MET, MET, MET, MET)
52 (PRO), 54 (TYR), 140 (PHE, PHE, PHE), 141 (LEU, LEU, LEU)
142 (ASN, ASN, ASN, ASN, ASN, ASN), 143 (GLY, GLY), 144 (SER, SER)
145 (CYS, CYS, CYS), 163 (HIS, HIS), 164 (HIS, HIS), 165 (MET, MET, MET)
166 (GLU, GLU, GLU, GLU, GLU), 167 (LEU, LEU), 168 (PRO), 172 (HIS)
187 (ASP, ASP, ASP, ASP), 189 (GLN, GLN, GLN), 190 (THR), 192 (GLN, GLN, GLN).

Analysis of ligand: Lipinski's Rule of Five in ADMET Lab 2.0

The Physiochemical properties including absorption, distribution, metabolism, excretion, and toxicity (ADMET) were analyzed based on Lipinki's rule of five. In the present research work, we have selected many herbal plants and their active bioactive compounds and studied

their drug-like property on ADMET Lab 2.0. The potential eleven bioactive compounds were selected, and the existing drugs like Dexamethasone, Redisivir, Zentamycine, and Neomycine were compared with them in various parameters. Lipinski's rule of five rejected some vital medicines like Azithromycine, Remdesivir, Neomycine, and Zentamycine which were already prescribed against Omicron and Deltacron and their subvariety in the pandemic.

Pharmacokinetic Analysis

For the drug-like soft rule, ligands should have a molecular weight of 100-600; however, some ligands like Neomycin and Polymyxin B1 have exceeded the parameters. Furthermore, the number of hydrogen bond donors and acceptors should be in the range of 0-7 and 0-12, but nHD & nHA analysis reveals that Neomycin, Polymyxin B1, Streptomycin, and Zantamycine have a high number of hydrogen donor and acceptors. So, their pharmacokinetic property is found abnormally high in many cases. The LogS (aqueous solubility value) represents the drug absorption process, the higher the value of logS better will be the oral dissolution. The LogP (Octanol/water distribution coefficient) represents the permeability of drugs and hydrophobic binding to macromolecules. Its value is considered proper in the range of 0-3. The HIA (Human intestinal Absorption) is a vital parameter for the apparent efficacy of drugs. The interpreted result has shown that the HIA > 30 % represents the poorly absorbed category (0) which is denoted by HIA (-), and < 30 % represents the category (1). The HIA should be in the range of 0-1, indicating 0-0.3 excellent (Green), 0.3-0.7 medium (Yellow), and 0.7-1 poor (++, Red). The Caco2 (Human colon Adenocarcinoma cell line, where drug absorption in vivo drug permeability is studied due to morphological and functional similarities. Its value should be -5.15 excellent (Green), and otherwise poor (Red). Great concern was given to the carcinogenicity in ADMET profiling due to its detrimental effect on the genome and metabolic processes. The empirical decision has revealed that category zero (non-carcinogenic) should have TD_{50} (0-0.3) considered an excellent drug (Green) (Lipinski, 2004).

Table 3. ADMET evaluation of different ligands based on Lipinski's rule of five.

Compound Name	PubChem ID	M.Wt 100-600	nHD 0~7	nHA 0~12	Log P 0~3 Mol/l	Max Ring 0~18	HIA	LogS > -4-0.5 Logmol/l	Caco-2 (cm/m)	Carcino density	Lipinski Rule
Withanone	21679027	470.6	2	6	1.874	18	---	-3.433	-5.014	0.839	Accepted
Azithromycin	447043	749	5	14	2.09	15	---	-2.472	-5.995	0.155	Rejected
Dexamethasone	5743	392.5	3	5	1.321	17	---	-3.509	-4.911	0.515	Accepted
Chloroquine	2719	319.9	1	3	4.733	10	---	-3.566	-4.981	0.204	Accepted
Remdesivir	56832906	531.2	8	18	-2.8	9	---	-1.979	-6.009	0.495	Rejected
Gallic acid	370	170.12	4	5	0.692	6	---	-1.55	-5.604	0.219	Accepted
Neomycin	8378	614.6	19	19	-2.581	6	+++	-0.431	-6.169	0.873	Rejected
Polymyxin B1	171395129	1237.5	23	29	0.331	23	+++	-2.705	-6.799	0	Rejected
Streptomycin	19649	581.6	16	19	-1.903	6	+++	-0.936	-6.178	0.05	Rejected
Gentamicin	3467	477.6	11	12	-0.168	6	+++	-1.403	-5.716	0.026	Rejected
Berberine	2353	336.4	0	5	3.12	21	---	-5.059	-5.01	0.808	Accepted
Palmatine	19009	352.4	0	5	2.893	18	+	-4.82	-5.042	0.655	Accepted
Magnoflorine	73337	342.4	2	5	0.863	16	+++	-2.613	-5.637	0.641	Accepted

Compound Name	PubChem ID	M.Wt 100-600	nHD 0~7	nHA 0~12	Log P 0~3 Mol/l	Max Ring 0~18	HIA	LogS > -4-0.5 Logmol/l	Caco-2 (cm/m)	Carcino density	Lipinski Rule
Tembetarine	167718	344.4	2	5	0.878	10	+++	-2.046	-5.619	0.198	Accepted
Choline	305	104.17	1	2	-1.293	0	+	0.559	-4.969	0.431	Accepted
Isocolumbin	24721165	358.4	1	6	1.189	5	--	-3.129	-4.683	0.793	Accepted
Tetrahydropalmatine	5417	355.4	0	5	1.89	18	---	-2.579	-4.671	0.843	Accepted

6LU7 M^{pro} and Ligand Docking in ADFR 1.1

Molecular docking was carried out in ADFR 1.0 software by loading the protein receptor pbdqt file and the docking box parameter was fitted for different dimensions. The spacing in the dimension was kept at 0.375 and smoothing at 4 for different 24 flexible residues. IUPAC Name of Withanone (1S,2S,4S,5R,10R,11S,14S,15S, 18S)-15-[(1R)-1-[(2R)-4,5-dimethyl-6-oxo-2,3-dihydropyran-2-yl]ethyl]-5,15-dihydroxy-10,14-dimethyl-3-oxapentacyclo[9.7.0.02,4.05, 10.014,18]octadec-7-en-9-one. The flexible reduces for Withanone ligands protein chains are A: PHE8, GLN83, ASN84, VAL104, ARG105, ILE106, GLN107, GLN110, THR111, PHE112, SER113, GLN127, MET130, ASN151, ILE152, SER158, ASP176, LEU177, GLU178, ASN180, TYR182, THR292, PHE294, ASP295. The computer pockets for a score were 300.45 and the peptide scoring function for ligand size was found 500. The water map was set by keeping the weight 0.60, and entropy was kept at -0.20 for all clusters larger than 1. The box parameter size was adjusted in the center X = -35.134, Y = 16.306, and Z = 60.027, similarly, the size was kept X= 9.000, Y= 9.00, and Z 9.500.

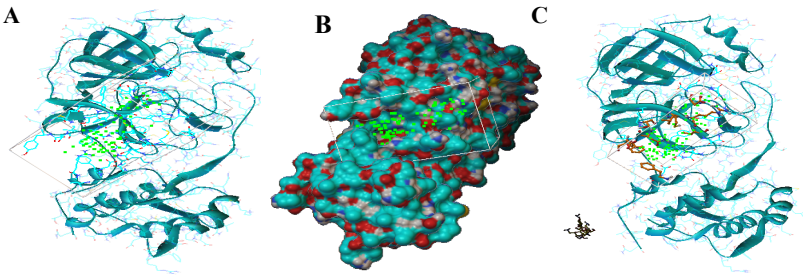

Fig. 3. Molecular docking of 6LU7 with Withanone ligand in AGFR 1.1

A. Clean M^{pro} of SARS-CoV-2 main protease 6LU7 showing higher AS core and active sites for docking.

B. Receptor surface showing possible docking sites in box representation before docking.

C. 24 different amino acid residues from ligand docked with amino acid residue in receptor surface after docking.

The interaction simulation of 2D and 3D structure reveals that the amino acid residue of Withanone interacts and forms conventional hydrogen bonding as A: GLN107:HE22 -: UNK0:O with hydrogen bonding 2.16272 Å, with DHA angle 149.226, HAY angle 112.707 and: UNK0:H - A: ARG105:O with hydrogen bonding 1.75976 Å, with DHA 161.086 and angle HAY 130.385. The amino acid residues VAL A: 104 and PHE A 294 also interact with ligands to form alkyl bonds with unstable and large bond angles. The interaction of the residue of Withanone with

protein receptors is very stable with minimum bond distance compared to the other ligand interactions. In our previous finding, we reported that the strong interaction of Withanone in the P53 signaling pathway as a potential inhibitor in 5TRF-P53 interaction, where Withanone played a pivotal role in apoptosis and provided a basis for modulating NF-kB and STA3 (S. R. Regmi *et al.*, 2024). Furthermore, the use of *Withania somnifera* in the pandemic shows its anti-cancerous activity, anti-inflammatory, antioxidant effect, neuroprotective effect, immunomodulatory effect, anti-aging, anti-stress, cardioprotective, hepatoprotective, antibacterial, and most effectively antiviral property against SARS-CoV-2. The countless mutation on the spike protein of SARS-CoV-2 shows that the ACE2 receptor of the host cell very is susceptible and can be interfered with only by the potential inhibitor which can defunct the interaction. The strong and stable hydrogen bonding of Withanone with Mpro of SARS-CoV-2 can terminate the RNA polymerase replication in the host cell.

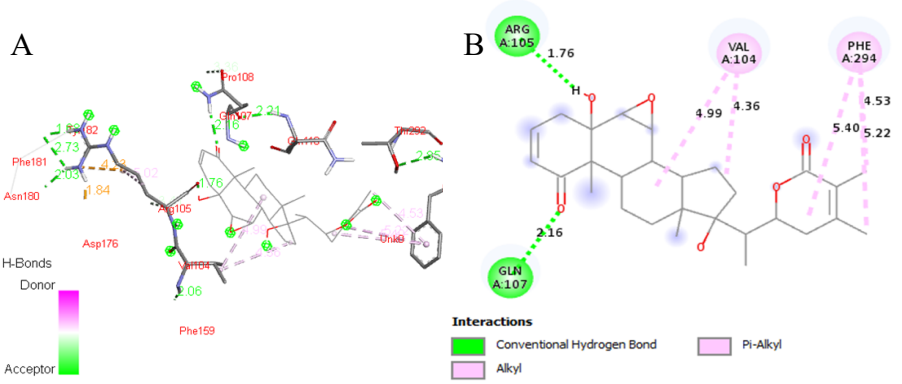

Fig. 4. Interactive visual representation of receptor-ligand docked complex in Discovery studio 21.0.

A. Visual representation of 3D interaction for Mpro SARS-CoV-2 with Withanone showing amino acid residue with ligand.

B. 2D interaction showing bond distance for conventional hydrogen bonding and other bonding between donor and acceptor

The stereochemical foundation of protein structure is analyzed by Ramachandran plot, which gives stability and indicates the purity of protein based on dihedral angle Phi (ϕ) and Psi (ψ). The stability of a protein is determined based on visualization of allowed and disallowed regions for their respective steric hindrance. The plot represents four quadrants I (0-90°), II (90-180°), III (180-270°), and IV (270-360°). The rotation of residue around N-Cα is denoted by X-axis angle Psi (ψ) and Y-axis Phi (ϕ) denotes the rotation of amino acid residue around C-αC. The shaded region in the plot represents the allowed region and the white area represents the disallowed region. The angle -120° to +120° represents the residue in β-sheets and quadrant I indicates the α-Helix of the protein. Each point in the plot represents a single residue, and quadrant II & III represent the secondary structure of the protein. The quadrant II represents the quality of protein; the maximum number of points on this quadrant depicts the higher quality of protein (Ramachandran, 1963; Richardson & Richardson, 1988; Lovell *et al.*,

2003; Laskowski *et al.*, 1993). The average hydrophobicity patterns of the docked complex are analyzed for the identification of amino acid sequences. The trend analysis shows that the peak in the graph depicts the hydrophobicity and the troughs show the hydrophilic region in the docked complex. The red peak, which shows hydrophobicity, represents the secondary protein structure, and the troughs region shows conventional hydrogen bonding. The extreme high and low peaks represent the active binding sites in the protein (Kyte & Doolittle, 1982), (Creighton, 1993).

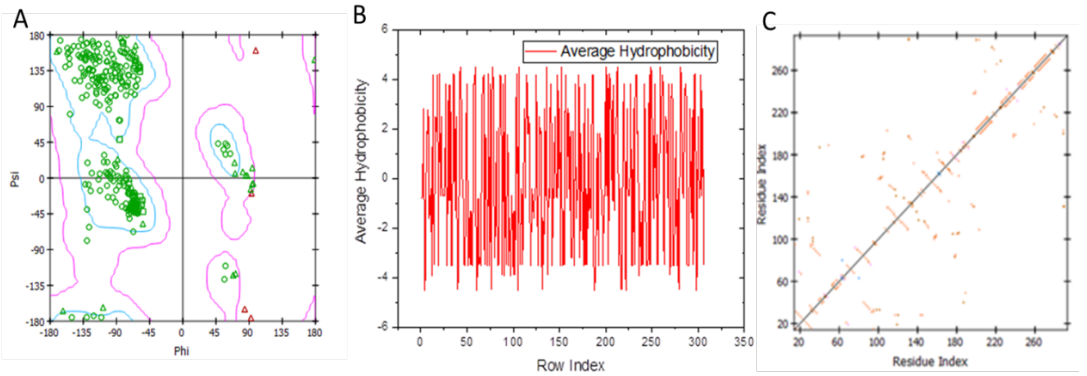

Fig. 5. 6LU7-Withanone docked complex analysis in Discovery studio.

A. *Ramachandran plot showing protein Phi(φ) stereochemistry vs. Psi(ψ).*
B. *Hydrophobicity of protein in docked complex.*
C. *Hydrogen bonding showing residue index for different active binding sites*

Remdesivir is an effective drug against SARS-CoV-2 infection during the pandemic. It was first launched to deactivate the replication of Ebola but its nucleotide analog product is widely used in broad-spectrum RNA replication of the virus. The report revealed that it is effective against lower respiratory tract infection related to COVID-19 infection (Beigel *et al.*, 2020) (Grein *et al.*, 2020). Remdesivir (GS-5734) is a mono-phosphoramidate drug, which terminates RNA replication effectively. Still, the pharmacokinetic study reveals that its absorption is poor with moderate plasma binding and inactive metabolism with high excretion. The targeted protein-ligand interaction depicts that SER A: 158 interacts with the ligand and gives the stable conventional hydrogen bonding 2.03 Å. Similarly, ARG A: 105 shows multiple interactions with ligands with bond distances of 1.89 Å and 1.83 Å. Furthermore, THR A: 292 interacts with the bond distance of 2.50 Å. However, its efficacy was reported more than 60% in clinical trials, the hypersensitivity, hepatoxicity, renal failure, and gastrointestinal problems kept its potential in doubt. According to the WHO, Remdesivir does not have any influence on reducing the mortality rate, however, some meta-analysis of multiple studies explores that it reduces the recovery time to some extent and prevents the patient's proximity towards ventilation. In contrast to the potential of Remdesivir, the Ayurveda medicine powder of *Withania somnifera* prescribed in India was found effective in several cases.

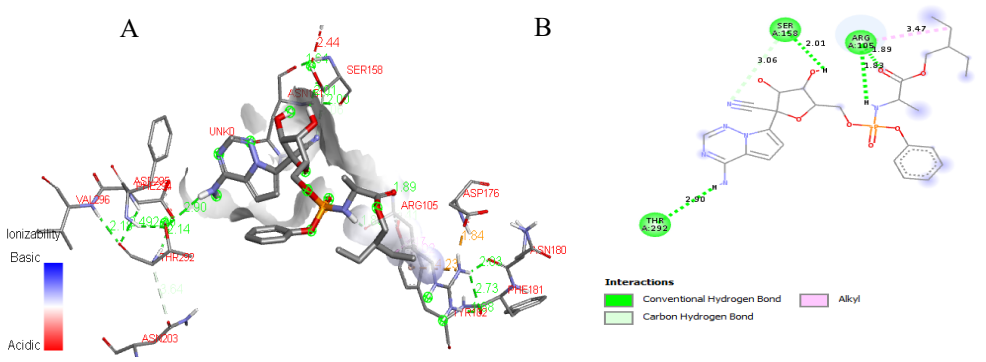

Fig. 6. Interactive visual representation of receptor-ligand docked complex in Discovery studio 21.0.

A. *Visual representation of 3D interaction for Mpro SARS-CoV-2 with Remdesivir showing amino acid residue with ligand.*

B. *2D interactive diagram showing the bond distance of hydrogen bonding and Alkyl bonding residue.*

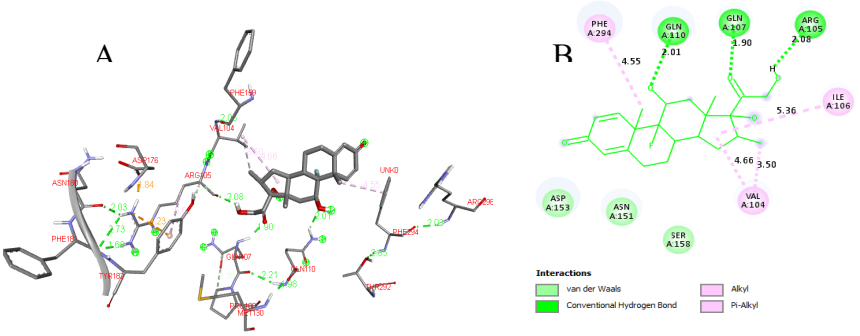

Fig. 7. Interactive visual representation of receptor-ligand docked complex in Discovery studio 21.0.

A. Visual representation of 3D interaction for M pro-SARS-CoV-2 with Dexamethasone showing amino acid residue with ligand.

B. 2D interactive diagram showing the bond distance of hydrogen bonding and Alkyl bonding residue.

Dexamethasone is a corticosteroid that got attention during the COVID-19 pandemic due to its anti-inflammatory properties. Reports have shown that it reduced the 33% mortality in COVID-19 cases due to its effectiveness against cytokinin storm that shows lung and muti-organs failure (Group, 2021), (Keyt, 2021). Molecular docking results for Dexamethasone and main protease show that ARG A:105 of protein residue makes a stable conventional hydrogen bonding with a bond distance of 2.08 Å, GLN A:107 makes 1.90 Å and GLN A: 110 with a bond distance of 2.01 Å. Dexamethasone shows relatively stable hydrogen bonding and docking score greater than Remdesivir.

Fig.6.

Table 4. Docking score of the Main protease of SARS-CoV-2 with different ligands and their maximum score. Docking score (Röhrig *et al.*, 2023) and (Bugnon *et al.*, 2024), individual docking score is calculated by Window power shell method.

Ligands	Withanone	Azithromycin	Dexamethaso	Chloroquine	Remdesivir	Gallic acid	Neomycin	Polymyxin B1	Streptomycin	Gentamycin	Berberine	Palmatine	Magnoflorine	Tembetarine	Choline	Isocolumbin	Tetrahydro palmatine
Free energy ($KCalMol^{-1}$)	-8.50	-7.47	-7.30	-7.74	-7.70	-5.96	-8.04	-8.15	-7.42	-7.02	-7.32	-7.28	-7.50	-7.32	-5.27	-7.77	-7.82

The molecular docking of the Main protease of SARS-CoV-2 with different ligands scores is shown in Table 4. The docking score was found high for Withanone -8.50 $KCalMol^{-1}$. Similarly, in the same parameters file by keeping fixed box size, nbRuns 8, and maxEvals 50000, 3C like proteinase nsp5, we have found the docking score for Azithromycin (-7.47 KCalMol-1), Dexamethasone (-7.30 KCalMol-1), Chloroquine (-7.74 $KCalMol^{-1}$), Remdesivir (-7.70 $KCalMol^{-1}$), Neomycin (-8.04 $KCalMol^{-1}$), Polymyxin B1(-8.15 $KCalMol^{-1}$), Streptomycin (-7.42 $KCalMol^{-1}$), Gentamycin (-7.02 $KCalMol^{-1}$), Berberine (-6.32$KCalMol^{-1}$), Palmtine (-7.28 $KCalMol^{-1}$), Magnoflorine(-7.50 $KCalMol^{-1}$), Tembetarine (-7.32 $KcalMol^{-1}$), Isocolumbin (-7.77 $KCalMol^{-1}$), Terahydropalmatine (-7.82 $KCalMol^{-1}$). The report shows that the HIV protease Nelfinavir has a strong docking score (-9.93 $KCalMol^{-1}$), and Lopinavir is also an HIV protease that shows a docking score (-8.86 KCalMol-1). An antiretroviral drug Ritonavir shows a docking score (-8.78 KCalMol-1). The antiviral drug Favipiravir shows a docking score (-7.0 $KCalMol^{-1}$). The HCV protease inhibitor shows a docking score (-9.93 $KCalMol^{-1}$), Indinavir (-9.70 $KCalMol^{-1}$), the antineoplastic agent Carmofur (-8.50 $KCalMol^{-1}$), (Ton *et al.*, 2020; Bhardwaj *et al.*, 2021; Pant *et al.*, 2021).

The high docking score reveals that the main protease M^{pro} of SARS-CoV-2 interacts very strongly with Withanone. The interactive residue ARG A: 105 and GLN A: 107 are very strongly bonded through conventional hydrogen bonding with the least possible and stable bond distances 1.76, and 2.16 Å. Comparing this stability with other ligands, none of the interactions can exceed the least possible distance of the 6LU7-Withanone complex. Furthermore, the drugs approved by WHO during the pandemic are promising in some sorts of circumstances but their docking score, bond distances, ADMET evaluation, and results in clinical trials are not much more satisfactory. The possibility of failure of these drugs in many cases could be the improper bonding of the main protease with ligands like Dexamethasone, Remdesivir, Hydroxychloroquine, and Polymyxin B1 formated salt, Azithromycin, Streptomycin, and Gentamycin. The WHO never recommended Remdesivir and Hydroxychloroquine in SARS-CoV-2 infection in the pandemic. Probably the reason is that the ACTT-1 trial of Remdesivir on the patient before the ventilation ultimately put them in jeopardy. However, the US government

prescribed Hydroxychloroquine in SARS-CoV-2 in serious cases; the mortality rate was increased significantly. In the severe painful situation of the pandemic, Dexamethasone was found promising in critical cases but reports show that we need to focus on an alternative effective drug that can terminate the propagation of Omicron main protease.

Table 5. Interaction of main protease SARS-CoV-2 with ligand showing all possible hydrogen bonding, interacting residue, and bond distance.

SARS-CoV-2 M^{pro} (ChainA)	Ligands	Interacting residue (Amino acids)	Number of Hydrogen bonding	Bond Distance (Å)
6LU7	Withanone	ARG A: 105, GLN A: 107	2	1.76, 2.16
	Dexamethazone	ARG A: 105, GLN A: 107,	3	2.08, 1.90
		GLN A: 110		2.01
	Chloroquine	GLN A: 110	1	2.47
	Remdesivir	ARG A: 105, SER A : 158	3	1.83, 2.01
		THR A: 292		2.90
	Neomycin	LYS A: 97, ASN A: 72, ASN A:119, GLY	6	2.35, 2.23, 2.72,
		120, SER A 121, MET A: 17		2.02, 2.11, 2.15
	Polymyxin B1	SER A: 113, VAL A: 114, LEU A: 115,		2.28, 2.45, 2.12,
		TYR A: 126, CYS A 128, ASN A 151	6	2.56, 2.08, 1.89
	Gentamicin	SER A:113, VAL A: 114, TYR:A 126, CYS	7	1.67, 2.14, 1.97,
		A:128, PHE A:150, ASN A:151, PHE A:8		2.32, 2.15, 2.24, 2.67
	Berberine	LEU A: 58, ILE A:60, LYS A:61, HIS A: 80	4	1.78, 1.98, 1.57, 1.97
	Palmatine	LYS A: 97, ASN A:95, GLY A:15, MET A:17	4	1.87, 2.32, 1.66, 2.43
	Magnoflorine	VAL A:20, VAL A:42, LEU A: 27, ASN	5	181, 2.36, 2.56, 2.13,
		A:28, CYS A:145		1.89
	Tembetarine	ASN A:214, ALA A:210, GLN A:256, VAL	4	2.13, 2.45, 2.47, 1.78
		A:296		
	Isocolumbin	GLN A:83, CYS A 85, ARG A 40, GLU A	5	2.45, 2.03, 2.15,
		178, GLY 197		2.14, 1.76
	Tetrahydropalmatine	HIS A:163, TYR A 161, THR A:175, GLY	6	1.78, 1.97, 2.13,
		A 174, MET A 162, SER A 147		1.87, 1.65, 1.78

Gentamycin was prescribed for secondary bacterial infection in COVID-19 cases but the molecular docking result shows that the amino acid residue of this drug forms stable hydrogen bonding with the main protease. Similarly, Berberine, Palmatine, Magnoflorine, Tembetarine, Isocolumbin, and Terahydropalmatile also show strong and stable hydrogen bonding with considerably significant docking scores.

Molecular Dynamics: Analysis of NAND, RMSD, and RMSF plots

The log file was generated with the help of a docked complex 'psf' file and solvation box in *VMD 1.9.4α53.* The NAMD plots were generated by Dell i5-11th gen 16GB DDR4RAM, 512 NVME SSD, 2.90GHz at GSST, MU. Results show that the 6LU7-Withanoe complex is stable. The conventional hydrogen bonding between receptor with ligand in ARD A: 105 with bond

angle 1.76 Å and GLN A: 107 with bond distance 2.16 Å does not change in a 100 ns time frame. Furthermore, the stereochemistry belonging to the dihedral angle does not change in the same time scale. The volume and pressure variation were found stable in the NAMD plot. Which confirms the stability of the 6LU7-Withanone docked complex.

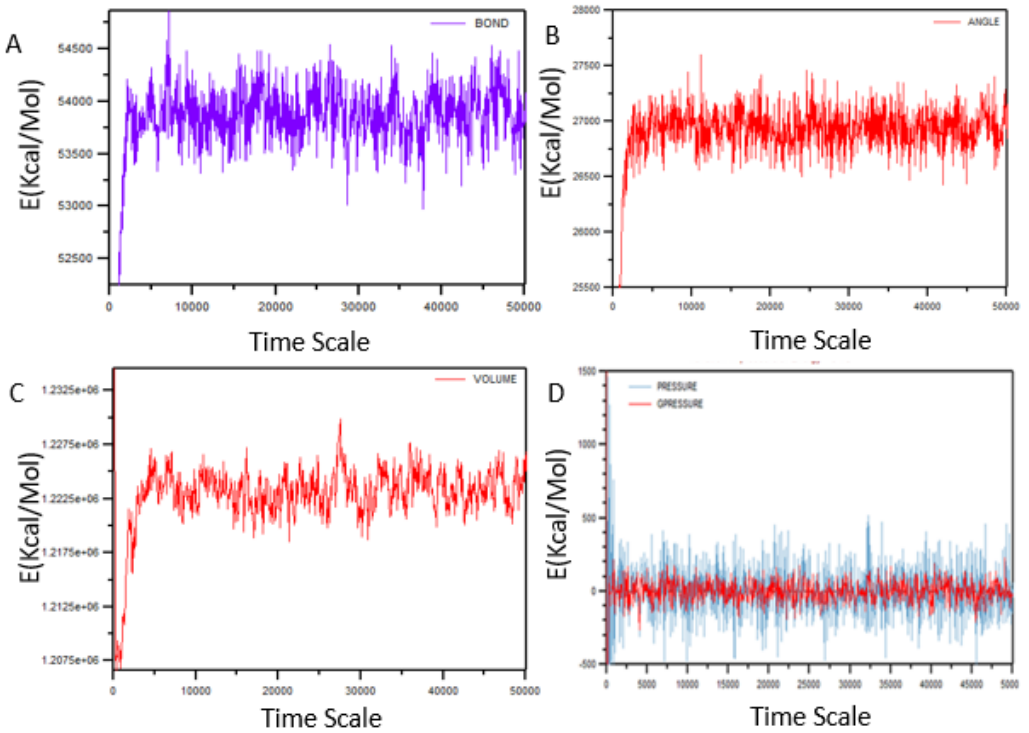

Fig. 8. NAMD plot for 6LU7-Withanone complex showing A) Energy vs. time scale for the stability of the bond. B) Energy vs. time scale for the stability of angle fluctuation. C) Volume variation for docked complex with time scale. D) Energy vs. time scale for the variation of PRESSAUG and GPRESSAUG.

The RMSD plot for the docked complex 6LU7-Withanone suggests the molecule has stable stereochemical confirmation. The docked complex is stable below 0.9 Å. A similar result was obtained for docked 6LU7-Tetrahydropalmatine. The stable confirmation of both complexes reveals the main protease is stabilized without fluctuation in the given 100 ns time frame.

The RMSF plot was obtained through the CABS-flex 2.0 online server for 10 ns. The maximum RMSF values for the 6LU7-Withanone complex are found below 4 Å. The residue index of 55 shows a fluctuation of 3.5 Å, the 105-residue index shows 2.75 Å and the 155 residue index is 3.33 Å. Similarly, the 175 and 180 residue indexes represent loops and flexible domains that show RMSF at 2.75 Å and 1.75 Å probably due to binding and conformational change. The

residue index 185 is the flexible termini that shows fluctuation at 3.5 Å. The other ligand like Remdesivir, Dexamethasone, and Hydroxychloroquine also shows stable RMSF below 5 Å but they show higher fluctuation in RMSD.

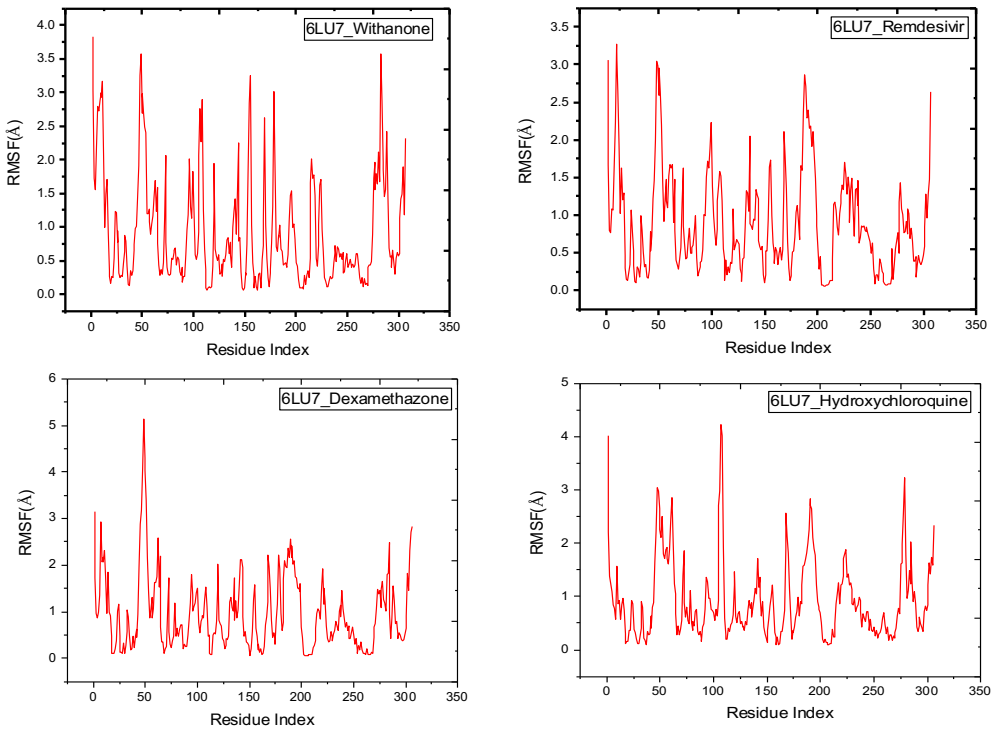

Fig. 9. RMSF plots for receptor-Ligand complex for 10ns time frame A) 6LU7-Withanone complex B) 6LU7-Remdesivir C) 6LU7-Dexamethazone and D) 6LU7-Hydroxychloroquine.

Conclusion

In silico molecular docking and dynamic were used in the present research work to determine the potential inhibitor against the main protease of SARs-CoV-2. The clean main protease was obtained through the refinement on PyMol and Avogadro software that was further investigated in CAST 2.0 for sequence study and determination of its various physical properties like volume, surface area, total number of residues in a particular chain, and maximum number of active sites. ADMET evaluation was performed for more than 400 bioactive compounds in ADMET lab 3.0, based on Lipinski's rule of five, and only some compounds having drug-like properties were chosen for the molecular docking. The Molecular docking was carried out in AGFR 1.1 software by keeping all possible parameters functional to get the highest docking score. It was found for Withanone (-8.50 $KCalMol^{-1}$), Azithromycin (-7.47 KCalMol-1), Dexamethasone (-7.30 KCalMol-1), Chloroquine (-7.74 $KCalMol^{-1}$), Remdesivir (-7.70 $KCalMol^{-1}$), Neomycin (-8.04 $KCalMol^{-1}$), Polymyxin B1 (-8.15 $KCalMol^{-1}$), Streptomycin (-7.42 $KCalMol^{-1}$),

Gentamycin(-7.02 KCalMol^{-1}), Berberine (-6.32 KCalMol^{-1}), Palmtine (-7.28 KCalMol^{-1}), Magnoflorine (-7.50 KCalMol^{-1}), Tembetarine (-7.32 KCalMol^{-1}), Isocolumbin (-7.77 KCalMol^{-1}), Terahydropalmatine (-7.82 KCalMol^{-1}). The interactive 2D and 3D diagram in Biovia Discovery studio reveals the strong interaction of Withanone with protein residue in ARG A: 105 and GLN A: 107 having bond distances of 1.76 and 2.16 Å that were found relatively stronger interaction than the medicine prescribed in COVID-19 pandemic. Furthermore, the result explores that Palmatine, Magnoflorine, Tembetarine, Isocolubin, and Tetrahydropalmitine also favor the formation of strong conventional hydrogen bonding. The stability of the docked complex was analyzed through NAMD, RMSD, and RMSF plots. The NAMD plot for the Protein Withanone complex depicts that its Root mean square deviation (RMSD) is less than 1Å. Similarly, its Root mean square fluctuation (RMSF) was found less than 5 Å. A similar result was obtained for the protein-Terahydropalmatine complex. Therefore, the molecular docking and dynamics imply that bioactive alkaloids Withanone, Tetrahydropalmatine, Magnoflorine, Tembertine, and Isocolumbin could be the possible candidates to inhibit the replication of SARS-CoV-2 main protease in the host cell.

Acknowledgments

The author would like to acknowledge Dr. Jhasanath Adhikari 'Subin' for his support and direction in the research work. Authors are also thankful to the Dean's office of the Graduate School of Science and Technology (GSST), Mid-West University.

Declaration

This research work does not have any kind of conflict of interest.

References

Abdullah Alharbi, R. (2021). Structure insights of SARS-CoV-2 open state envelope protein and inhibiting through active phytochemical of ayurvedic medicinal plants from Withania somnifera. *Saudi Journal of Biological Sciences*, *28*(6). https://doi.org/10.1016/j.sjbs.2021.03.036

Ahmad, S. U., Hafeez Kiani, B., Abrar, M., Jan, Z., Zafar, I., Ali, Y., Alanazi, A. M., Malik, A., Rather, M. A., Ahmad, A., & Khan, A. A. (2022). A comprehensive genomic study, mutation screening, phylogenetic and statistical analysis of SARS-CoV-2 and its variant omicron among different countries. *Journal of Infection and Public Health*, *15*(8). https://doi.org/10.1016/j.jiph.2022.07.002

Alam, S., Sarker, M. M. R., Afrin, S., Richi, F. T., Zhao, C., Zhou, J. R., & Mohamed, I. N. (2021). Traditional Herbal Medicines, Bioactive Metabolites, and Plant Products Against COVID-19: Update on Clinical Trials and Mechanism of Actions. In *Frontiers in Pharmacology* (Vol. 12). https://doi.org/10.3389/fphar.2021.671498

Altooq, N., Humood, A., Alajaimi, A., Alenezi, A. F., Janahi, M., AlHaj, O., & Jahrami, H. (2022). The role of micronutrients in the management of COIVD-19 and optimizing vaccine efficacy. In *Human Nutrition and Metabolism* (Vol. 27). https://doi.org/10.1016/j.hnm.2022.200141

Balkrishna, A., Bhatt, A. Ben, Singh, P., Haldar, S., & Varshney, A. (2021). Comparative retrospective open-label study of ayurvedic medicines and their combination with allopathic drugs on asymptomatic and mildly-symptomatic COVID-19 patients. *Journal of Herbal Medicine*, *29*. https://doi.org/10.1016/j.hermed.2021.100

472

Bayani, F., Hashkavaei, N. S., Arjmand, S., Rezaei, S., Uskoković, V., Alijanianzadeh, M., Uversky, V. N., Ranaei Siadat, S. O., Mozaffari-Jovin, S., & Sefidbakht, Y. (2023). An overview of the vaccine platforms to combat COVID-19 with a focus on the subunit vaccines. In *Progress in Biophysics and Molecular Biology* (Vol. 178). https://doi.org/10.1016/j.pbiomolbio.2023.02.004

Beigel, J. H., Tomashek, K. M., Dodd, L. E., Mehta, A. K., Zingman, B. S., Kalil, A. C., Hohmann, E., Chu, H. Y., Luetkemeyer, A., & Kline, S. (2020). Remdesivir for the treatment of Covid-19—preliminary report. *New England Journal of Medicine*, *383*(19), 1813–1836.

Bhardwaj, V. K., Singh, R., Sharma, J., Rajendran, V., Purohit, R., & Kumar, S. (2021). Identification of bioactive molecules from tea plant as SARS-CoV-2 main protease inhibitors. *Journal of Biomolecular Structure and Dynamics*, *39*(10), 3449–3458.

Brant, A. C., Tian, W., Majerciak, V., Yang, W., & Zheng, Z.-M. (2021). SARS-CoV-2: from its discovery to genome structure, transcription, and replication. *Cell & Bioscience*, *11*, 1–17.

Bugnon, M., Röhrig, U. F., Goullieux, M., Perez, M. A. S., Daina, A., Michielin, O., & Zoete, V. (2024). SwissDock 2024: major enhancements for small-molecule docking with Attracting Cavities and AutoDock Vina. *Nucleic Acids Research*, gkae300.

Creighton, T. E. (1993). *Proteins: structures and molecular properties*. Macmillan.

Dong, E., Ratcliff, J., Goyea, T. D., Katz, A., Lau, R., Ng, T. K., Garcia, B., Bolt, E., Prata, S., & Zhang, D. (2022). The Johns Hopkins University Center for Systems Science and Engineering COVID-19 Dashboard: data collection process, challenges faced, and lessons learned. *The Lancet Infectious Diseases*, *22*(12), e370–e376.

Grein, J., Ohmagari, N., Shin, D., Diaz, G., Asperges, E., Castagna, A., Feldt, T., Green, G., Green, M. L., & Lescure, F.-X. (2020). Compassionate use of remdesivir for patients with severe Covid-19. *New England Journal of Medicine*, *382*(24), 2327–2336.

Group, R. C. (2021). Dexamethasone in hospitalized patients with Covid-19. *New England Journal of Medicine*, *384*(8), 693–704.

Hanwell, M. D., Curtis, D. E., Lonie, D. C., Vandermeersch, T., Zurek, E., & Hutchison, G. R. (2012). Avogadro: an advanced semantic chemical editor, visualization, and analysis platform. *Journal of Cheminformatics*, *4*, 1–17.

Jin, Z., Du, X., Xu, Y., Deng, Y., Liu, M., Zhao, Y., Zhang, B., Li, X., Zhang, L., & Peng, C. (2020). Structure of Mpro from SARS-CoV-2 and discovery of its inhibitors. *Nature*, *582*(7811), 289–293.

Jindal, D., & Rani, V. (2023). In Silico Studies of Phytoconstituents from Piper longum and Ocimum sanctum as ACE2 and TMRSS2 Inhibitors: Strategies to Combat COVID-19. *Applied Biochemistry and Biotechnology*, *195*(4). https://doi.org/10.1007/s12010-022-03827-6

Keyt, H. (2021). WHO recommends corticosteroids for patients with severe or critical COVID-19. *Annals of Internal Medicine*, *174*(1), JC2.

Krishnan, A., Hamilton, J. P., Alqahtani, S. A., & A. Woreta, T. (2021). A narrative review of coronavirus disease 2019 (COVID-19): clinical, epidemiological characteristics, and systemic manifestations. *Internal and Emergency Medicine*, *16*, 815–830.

Kyte, J., & Doolittle, R. F. (1982). A simple method for displaying the hydropathic character of a protein. *Journal of Molecular Biology*, *157*(1), 105–132.

Laskowski, R. A., MacArthur, M. W., Moss, D. S., & Thornton, J. M. (1993). PROCHECK: a program to check the stereochemical quality of protein structures. *Journal of Applied Crystallography*, *26*(2), 283–291.

Lipinski, C. A. (2004). Lead-and drug-like compounds: the rule-of-five revolution. *Drug Discovery Today: Technologies*, *1*(4), 337–341.

Lovell, S. C., Davis, I. W., Arendall III, W. B., De Bakker, P. I. W., Word, J. M., Prisant, M. G., Richardson, J. S., & Richardson, D. C. (2003). Structure validation by Cα geometry: φ, ψ and Cβ deviation. *Proteins: Structure, Function, and Bioinformatics*, *50*(3), 437–450.

Lubin, J. H., Markosian, C., Balamurugan, D., Pasqualini, R., Arap, W., Burley, S. K., & Khare, S. D. (2021). Structural models of SARS-CoV-2 Omicron variant in complex with ACE2 receptor or antibodies suggest altered binding interfaces. *BioRxiv*.

Markosian, C., Staquicini, D. I., Dogra, P., Dodero-Rojas, E., Lubin, J. H., Tang, F. H. F., Smith, T. L., Contessoto, V. G., Libutti, S. K., & Wang, Z. (2022). Genetic and structural analysis of SARS-CoV-2 spike protein for universal epitope selection. *Molecular Biology and Evolution*, *39*(5), msac091.

Mousavizadeh, L., & Ghasemi, S. (2021). Genotype and phenotype of COVID-19: Their roles in pathogenesis. In *Journal of Microbiology, Immunology and Infection* (Vol. 54, Issue 2). https://doi.org/10.1016/j.jmii.2020.03.022

Nakagami, H. (2021). Development of COVID-19 vaccines utilizing gene therapy technology. *International Immunology*, *33*(10). https://doi.org/10.1093/intimm/dxab013

Ou, J., Lan, W., Wu, X., Zhao, T., Duan, B., Yang, P., Ren, Y., Quan, L., Zhao, W., Seto, D., Chodosh, J., Luo, Z., Wu, J., & Zhang, Q. (2022). Tracking SARS-CoV-2 Omicron diverse spike gene mutations identifies multiple inter-variant recombination events. *Signal Transduction and Targeted Therapy*, *7*(1). https://doi.org/10.1038/s41392-022-00992-2

Pant, S., Singh, M., Ravichandiran, V., Murty, U. S. N., & Srivastava, H. K. (2021). Peptide-like and small-molecule inhibitors against Covid-19. *Journal of Biomolecular Structure and Dynamics*, *39*(8), 2904–2913.

Regmi, S., Ghimire, K. N., Pokhrel, M. R., & Khadka, D. B. (2015). Adsorptive removal and recovery of aluminium (III), iron (II), and chromium (VI) onto a low cost functionalized phragmities karka waste. *Journal of Institute of Science and Technology*, *20*(2), 145–152.

Regmi, S. R., Sawd, N. P., Khan, N. H., & Joshi, P. R. (2024). In silico Molecular Docking and Dynamic Study of MDM2-p53 Inhibitor Alkaloids Extracted from Withania somnifera Against Tumor Growth. *KMC Journal*, *6*(2), 273–297. https://doi.org/10.3126/kmcj.v6i2.68906

Richardson, J. S., & Richardson, D. C. (1988). Amino acid preferences for specific locations at the ends of α helices. *Science*, *240*(4859), 1648–1652.

Röhrig, U. F., Goullieux, M., Bugnon, M., & Zoete, V. (2023). Attracting Cavities 2.0: Improving the Flexibility and Robustness for Small-Molecule Docking. *Journal of Chemical Information and Modeling*, *63*(12), 3925–3940. https://doi.org/ 10.1021/acs.jcim.3c00054

Sarkar, P. K., & Das Mukhopadhyay, C. (2021). Ayurvedic metal nanoparticles could be novel antiviral agents against SARS-CoV-2. In *International Nano Letters* (Vol. 11, Issue 3). https://doi.org/10.1007/s40089-020-00323-9

Shree, P., Mishra, P., Selvaraj, C., Singh, S. K., Chaube, R., Garg, N., & Tripathi, Y. B. (2022). Targeting COVID-19 (SARS-CoV-2) main protease through active phytochemicals of ayurvedic medicinal plants–Withania somnifera(Ashwagandha), Tinospora cordifolia (Giloy) and Ocimum sanctum (Tulsi)–a molecular docking study. *Journal of Biomolecular Structure and Dynamics*, *40*(1). https://doi.org/10.1080/07391102. 2020.1810778

Tian, W., Chen, C., Lei, X., Zhao, J., & Liang, J. (2018). CASTp 3.0: computed atlas of surface topography of proteins. *Nucleic Acids Research*, *46*(W1), W363–W367.

Ton, A., Gentile, F., Hsing, M., Ban, F., & Cherkasov, A. (2020). Rapid identification of potential inhibitors of SARS-CoV-2 main protease by deep docking of 1.3 billion compounds. *Molecular Informatics*, *39*(8), 2000028.

Weng, Y., Li, C., Yang, T., Hu, B., Zhang, M., Guo, S., Xiao, H., Liang, X.-J., & Huang, Y. (2020). The challenge and prospect of mRNA therapeutics landscape. *Biotechnology Advances*, *40*, 107534.

Wrapp, D., Wang, N., Corbett, K. S., Goldsmith, J. A., Hsieh, C.-L., Abiona, O., Graham, B. S., & McLellan, J. S. (2020). Cryo-EM structure of the 2019-nCoV spike in the prefusion conformation. *Science*, *367*(6483), 1260–1263.

Xiong, G., Wu, Z., Yi, J., Fu, L., Yang, Z., Hsieh, C., Yin, M., Zeng, X., Wu, C., & Lu, A. (2021). ADMETlab 2.0: an integrated online platform for accurate and comprehensive predictions of ADMET properties. *Nucleic Acids Research*, *49*(W1), W5–W14.

Yadav, R., Chaudhary, J. K., Jain, N., Chaudhary, P. K., Khanra, S., Dhamija, P., Sharma, A., Kumar, A., & Handu, S. (2021). Role of structural and non-structural proteins and therapeutic targets of SARS-CoV-2 for COVID-19. *Cells*, *10*(4), 821.

Yasamineh, S., Kalajahi, H. G., Yasamineh, P., Yazdani, Y., Gholizadeh, O., Tabatabaie, R., Afkhami, H., Davodabadi, F., farkhad, A. K., Pahlevan, D., Firouzi-Amandi, A., Nejati-Koshki, K., & Dadashpour, M. (2022). An overview on nanoparticle-based strategies to fight viral infections with a focus on COVID-19. In *Journal of Nanobiotechnology* (Vol. 20, Issue 1). https://doi.org/10.1186/s12951-022-01625-0

攀苏. (1963). Stereochemistry of polypeptide chain configurations.“. *J. Mol. Biol*, *7*, 95–99.